Optics Letters

Dispersion-engineered multi-pass cell for single-stage post-compression of an ytterbium laser

Laura Silletti,[1,*] Ammar bin Wahid,[1] Esmerando Escoto,[2] Prannay Balla,[2,3,4] Supriya Rajhans,[2,5] Katinka Horn,[6,7] Lutz Winkelmann,[2] Vincent Wanie,[1] Andrea Trabattoni,[1,8] Christoph M. Heyl,[2,3,4] and Francesca Calegari[1,9,10]

[1]Center for Free-Electron Laser Science CFEL, Deutsches Elektronen-Synchrotron DESY, Notkestr. 85, 22607 Hamburg, Germany
[2]Deutsches Elektronen-Synchrotron DESY, Notkestr. 85, 22607 Hamburg, Germany
[3]Helmholtz-Institut Jena, Fröbelstieg 3, 07743 Jena, Germany
[4]GSI Helmholtzzentrum für Schwerionenforschung GmbH, Planckstraße 1, 64291 Darmstadt, Germany
[5]Friedrich-Schiller-Universität Jena, Max-Wien-Platz 1, 07743 Jena, Germany
[6]Department of Chemistry and Applied Biosciences, Laboratory of Physical Chemistry, ETH Zürich, Vladimir-Prelog-Weg 2, 8093 Zürich, Switzerland
[7]Center for Molecular and Water Science CMWS, Deutsches Elektronen-Synchrotron DESY, Notkestr. 85, 22607 Hamburg, Germany
[8]Institute of Quantum Optics, Leibniz University Hannover, Welfengarten 1, 30167 Hannover, Germany
[9]The Hamburg Centre for Ultrafast Imaging, Universität Hamburg, Luruper Chaussee 149, 22761 Hamburg, Germany
[10]Institut für Experimentalphysik, Universität Hamburg, Luruper Chaussee 149, 22761 Hamburg, Germany
*laura.silletti@desy.de

Received 28 September 2022; revised 22 February 2023; accepted 23 February 2023; posted 1 March 2023; published 28 March 2023

Post-compression methods for ultrafast laser pulses typically face challenging limitations, including saturation effects and temporal pulse breakup, when large compression factors and broad bandwidths are targeted. To overcome these limitations, we exploit direct dispersion control in a gas-filled multi-pass cell, enabling, for the first time to the best of our knowledge, single-stage post-compression of 150 fs pulses and up to 250 µJ pulse energy from an ytterbium (Yb) fiber laser down to sub-20 fs. Dispersion-engineered dielectric cavity mirrors are used to achieve nonlinear spectral broadening dominated by self-phase modulation over large compression factors and bandwidths at 98% throughput. Our method opens a route toward single-stage post-compression of Yb lasers into the few-cycle regime.

https://doi.org/10.1364/OL.476846

Ytterbium (Yb)-based laser systems are playing an increasingly important role in the field of ultrafast science. In contrast to Ti:sapphire (Ti:Sa) laser systems, Yb-based lasers are power scalable into the kilowatt (kW) regime while operating at high repetition rates [1], making them a valuable tool not only for average power-demanding applications, but also for improving the signal-to-noise ratio of laser-based experiments. However, amplifier gain bandwidth as well as gain-narrowing effects typically limit their pulse duration to >100 fs. A route to overcome this limitation is the use of spectral broadening techniques with subsequent post-compression, allowing for the generation of few-cycle pulses with energies reaching far into the mJ regime [2–5]. In this context, gas-filled or solid-state-based multi-pass cells (MPCs) have emerged as a promising alternative to the more conventional hollow-core fiber (HCF) technique, as they support high efficiency, great energy scaling options, low beam pointing susceptibility, and compact setups [5,6]. Using a single-stage MPC, post-compression of Yb lasers to about 30 fs has already been demonstrated with an overall transmission exceeding 96% [4,7]. Recently, various attempts have been made to enable the direct compression of Yb lasers into the few-cycle regime [8,9]; for instance, a double-stage approach has been used to achieve the compression of 1.2 ps pulses down to 13 fs. This result has not only been achieved in a cascaded arrangement of long MPC setups, but also with the use of metallic cavity mirrors to support a sufficient spectral bandwidth, causing significant losses. Other recent approaches use cascaded post-compression schemes employing multiple stages [10] as well as fiber-based modal mixing schemes [11].

An important asset to mitigate the general limitations of spectral broadening, such as peak power degradation, self-steepening, or temporal pulse breakup, is the direct control of dispersion and nonlinearity, determining the dispersion length L_D and nonlinear length L_N as defined, e.g., in Refs. [12] and [13], respectively. The ratio between these two quantities L_D/L_N determines the broadening regime. For $L_D/L_N >> 1$, the pulse spreads quickly in time and the broadening process saturates. In contrast, for $L_D/L_N << 1$, i.e., approaching a dispersion-free or dispersion-balanced regime, self-phase modulation (SPM) dominates and new frequencies are generated very efficiently without a severe impact on the temporal pulse shape. Dispersion control has been exploited, e.g., in bandgap hollow-core photonic crystal fibers (HC-PCFs) by means of gas pressure gradients [14,15] or using Kagomé-type structured fibers. In fact, spectra supporting sub-10-fs pulses have been demonstrated; however,

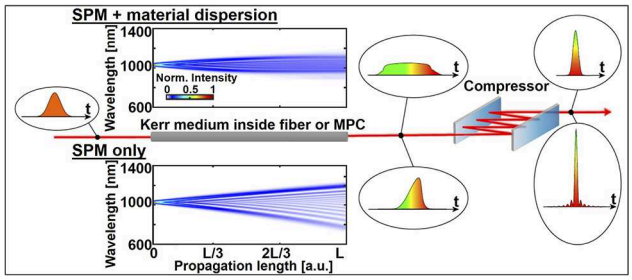

Fig. 1. SPM-based spectral broadening in a normal dispersive medium (top) and a dispersion-balanced scheme (bottom). The simulated SPM-based spectral evolution over the Kerr medium length L and the corresponding temporal pulse intensity profiles before and after compression are shown. In both cases, the simulations were performed considering an input pulse duration of 150 fs.

at low pulse energy and at the cost of low energy transmission [16,17]. Additionally, when targeting large compression factors and a broad bandwidth, dispersion-balanced regimes are difficult to reach with fiber-based spectral broadening methods. Here, MPCs can offer a solution, supporting dispersion control and therefore enabling SPM-dominated spectral broadening over large parameter ranges.

In this Letter, we exploit a post-compression method to approach the few-cycle regime with Yb-laser input pulses by using a single gas-filled MPC made of dispersion-engineered dielectric mirrors. We spectrally broaden and post-compress 122 µJ pulses at 1 kHz repetition rate and 150 fs input pulse duration down to 16 fs in a compact (400 mm length) MPC. To overcome limitations set by gas ionization, we optimize the group delay dispersion (GDD) inside the MPC, allowing the compression of 250 µJ pulses while preserving the spectral broadening characteristics, resulting in post-compressed pulses of 17 fs.

To illustrate the effect of dispersion control on the nonlinear spectral broadening process, we compare two different spectral broadening scenarios, considering the same input parameters for both examples, i.e., pulses with 150 fs duration centered at 1030 nm (Fig. 1). In the case of beam propagation through a conventional waveguide, e.g., a gas-filled HCF or MPC made of non-dispersive dielectric mirrors, the broadening process gets saturated rapidly and exhibits strong temporal pulse reshaping. However, in the case of an idealized fully dispersion-balanced waveguide, SPM-like spectral broadening is achieved over a larger bandwidth while showing only minor temporal pulse reshaping. This enables shorter pulse durations and higher peak intensities, albeit with weak temporal pre- and post-pulses typical of pure SPM [18]. Note that the temporal pulse structure can be cleaner in the first case, as discussed in earlier works [19].

Negatively chirped dielectric cell mirrors have been previously used within a solid-state-based MPC for achieving self-compression exploiting the anomalous dispersion regime [20]. However, this approach is limited by the peak intensity, which can easily reach the damage threshold of the nonlinear material or the anti-reflection coatings. Here, we instead exploit dispersion management for optimizing the spectral broadening process while utilizing high-pressure gases to circumvent the limitation imposed by bulk materials. Via numerical simulations based on a 3D propagation model [21], we investigate different MPC dispersion configurations mimicking the input parameters used for the experiments presented in this work.

As SPM-based spectral broadening is highly dependent on the input pulse shape, the pulse used in the simulations is characterized from the actual laser system to be used in the experiment. The beam profile is assumed to be Gaussian, as strong spatio-spectral effects are not expected in MPCs. In the case of a conventional MPC system employing low-GDD quarter-wave stack multi-layer mirrors and considering an input pulse duration of 150 fs at 250 µJ, our simulations predict a transform-limited (TL) output pulse duration of 21.4 fs (Fig. 2, setup 1). In contrast, for a dispersion-balanced MPC (dispersion: − 30 fs^2 per mirror bounce, pulse energy: 122 µJ), the theoretical prediction indicates a significantly broader spectral bandwidth corresponding to a TL of 11.8 fs (Fig. 2, setup 2). Using only a single dispersive mirror results in a TL of 13.3 fs (Fig. 2, setup 3). For all three configurations, the gas pressure was chosen so as to maximize the spectral broadening within the experimentally supported pressure range while maintaining low transmission losses. While setups 1 and 2 represent dispersion regimes with overall positive (setup 1) and negative (setup 2) dispersion, setup 2 supports a dispersion-balanced scenario. Thereby, both the gas density and the mirror coating determine the overall dispersion regime. Adjusting these two parameters enables us to tune the pulse energy while maintaining similar spectral broadening characteristics. This parameter tuning is typically limited by experimental setup constraints as well as ionization setting constraints in setup 2, where self-compression leads to ionization, thus limiting the maximum pulse energy. Note that the simulations include the specifications of the mirror coatings and that the negatively chirped mirrors cover a larger bandwidth than the low-GDD ones (see Supplement 1). Following our numerical predictions, we experimentally tested the feasibility of our concept. As displayed in Fig. 2, the overall experimental setup consists of a mode-matching lens telescope, a single-stage gas-filled MPC placed inside an overpressure chamber, and a chirped-mirror compressor. We employ a commercial Yb-doped fiber laser system (Tangerine, Amplitude) with a nominal pulse duration of 150 fs and a center wavelength of 1030 nm. The pulse energy can be tuned up to 250 µJ at 1 kHz repetition rate with a measured $M^2_{x,y}$ of 1.26×1.23. The laser pulses are coupled into a compact high-pressure chamber containing two 2" concave dielectric mirrors with a radius of curvature (ROC) R = -200 mm that are arranged in a Herriott-type configuration [22] about L = 400 mm in length, i.e., an L/R ratio of roughly 1.98. Two lenses with focal lengths of −150 mm and 250 mm, respectively, are used to match the laser beam to the eigenmode of the cell. In- and outcoupling of the beam are realized through a small rectangular (5 mm × 25.4 mm) dielectric mirror placed in front of one of the cell mirrors. The beam is recollimated by a spherical mirror and sent to a chirped-mirror compressor.

To achieve nonlinear spectral broadening inside the MPC, we distinguish between a conventional and a dispersion-controlled configuration. In the first case, (Fig. 2, setup 1) standard quarter-wave stack mirrors are used in 1.4 bar krypton and the beam is aligned for 22 round trips through the MPC. The pulse is post-compressed by means of two broadband dispersion-compensating mirrors (DCMs) to compensate for about 1850 fs^2 of positive GDD acquired during the nonlinear process and an additional 8 mm of fused silica glass. In the second case, dispersion-engineered dielectric cell mirrors are employed as MPC mirrors. Two cell mirrors, each with a GDD of -30 fs^2, are used to compensate for linear dispersion during a single pass through the cavity at 2.7 bar krypton and a total of 15 round trips

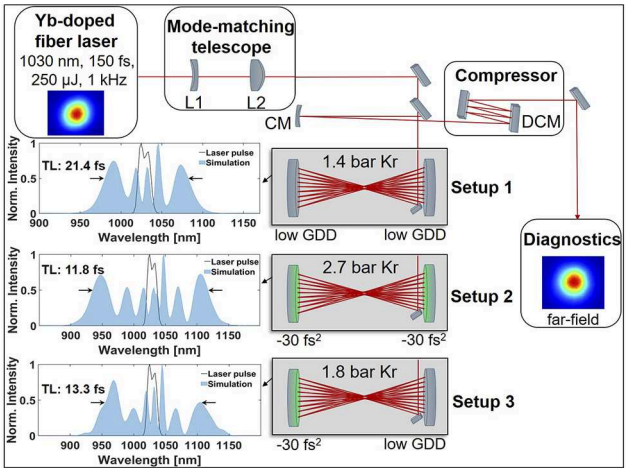

Fig. 2. Schematic of the overall pulse compression setup composed of a mode-matching lens telescope (L1: concave lens and L2: convex lens), a gas-based single-stage MPC, a spherical mirror (CM: concave mirror) for collimation, and dispersion-compensating mirrors (DCMs) for post-compression. We distinguish between three different MPC setups: setup 1 is based on two low-GDD cell mirrors, setup 2 incorporates two dispersive cell mirrors, and setup 3 consists of one dispersive and one low-GDD cell mirror. Numerical results are displayed for setup 1, setup 2, and setup 3.

through the MPC (Fig. 2, setup 2). Post-compression is achieved by employing a broadband DCM pair to compensate for roughly 800 fs^2 during propagation inside the MPC.

While for Setup 1 the full laser pulse energy (250 uJ) is coupled into the MPC, Setup 2 can only support half of the pulse energy (122 uJ) since the employed dispersive mirrors cause phase overcompensation, and the resulting increased intensity induces ionization. This limit can be easily overcome by reducing the gas pressure to 1.8 bar and by replacing one of the −30 fs^2 mirrors by a low-GDD one (see setup 3 in Fig. 2), resulting in an approximately dispersion-balanced scenario. Pulse compression is achieved via the same broadband DCM pair, which now compensates for a GDD of approximately 600 fs^2. Note that a further loss of 8% of the pulse energy is measured after the compressor mirrors. The spectra generated from setups 2 and 3 are acquired with two different spectrometers, Ocean FX and NirQuest by Ocean Insight Inc., in order to detect the full spectral range. A second-harmonic frequency-resolved optical gating (SH-FROG) setup is used to characterize the generated pulses for each configuration. For setup 1, we reconstruct a pulse duration of 22 fs, in agreement with the transform limit of 21.7 fs (FWHM) of the spectrum represented by the red curve in Fig. 3(a). As explained above, here, pulse duration and spectral broadening are not only limited by the bandwidth of the employed low-GDD dielectric cell mirrors but also, most importantly, by the interplay between the linear dispersion of the gas and SPM, leading to broadening saturation.

In contrast, controlling the GDD inside the MPC results in significant additional spectral broadening while maintaining a throughput as high as 98% measured directly at the MPC output. A spectral bandwidth of approximately 130 nm (FWHM) is measured, corresponding to a TL of 12.4 fs at FWHM [Fig. 3(a), blue-filled curve]. This is in agreement with the predictions from the numerical simulations. The pulses are characterized and post-compressed down to 16.4 fs with a FROG error of approx.

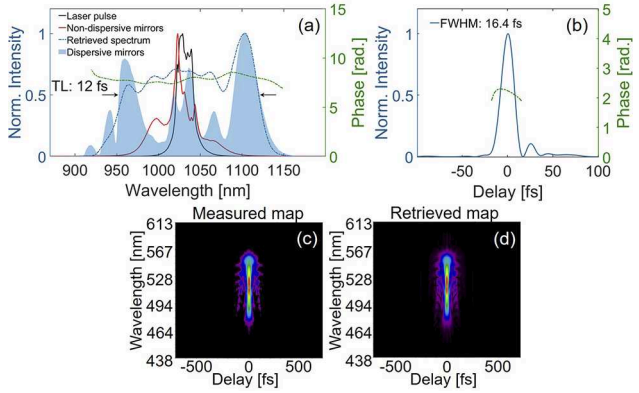

Fig. 3. Output pulse characteristics of setup 2. (a) Spectral comparison between the laser pulse (black), setup 1 (red), setup 2 (blue-filled), and the corresponding FROG-retrieved spectrum (dashed blue) and phase (dashed green). (b) FROG-retrieved temporal profile (blue) and phase (dashed green). (c) Measured and (d) retrieved FROG traces.

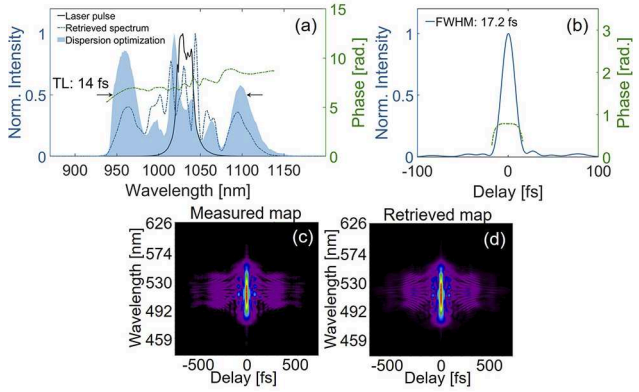

Fig. 4. Output pulse characteristics of setup 3. (a) Spectral comparison between the laser pulse (black), setup 3 (blue-filled), and its FROG-retrieved spectrum (dashed blue) and phase (dashed green). (b) FROG-retrieved temporal profile (blue) and phase (dashed green). (c) Measured and (d) retrieved FROG traces.

0.2%. Both the measured and retrieved FROG traces [Figs. 3(c) and 3(d)] as well as the retrieved pulse duration [Fig. 3(b)] show residual third-order dispersion. This can be attributed to the DCMs, which are not fully optimized for the measured spectral phase. We assign the disagreement between the retrieved and the experimentally measured spectra to the limited dynamic range of our FROG measurements, which prevented the accurate phase retrieval of possible temporal pulse pedestals with spectral content around the central wavelength. Moreover, the asymmetry of the generated spectrum on the blue side clearly indicates that the cell mirror coating is imposing a limit on the maximum achievable broadening. While only half of the laser energy can be used in setup2, setup 3 can be operated with the full laser energy (250 µJ) while still maintaining an MPC throughput of more than 90%. Furthermore, the generated spectral bandwidth is preserved and corresponds to a TL of 13.9 fs [Fig. 4(a), blue-filled curve]. The sharp cut of the spectrum on the blue side can again be attributed to the bandwidth limits of the cell mirror coating. The FROG-retrieved temporal profile [Fig. 4(b)] shows compression to 17.2 fs FWHM with a FROG

error of approx. 0.3%. Recently, we performed tests at 200 kHz repetition rate, corresponding to 50 W average power, indicating that the spectral broadening is preserved while maintaining an MPC throughput of >90% (see Supplement 1).

In conclusion, we have demonstrated the potential of direct dispersion control in MPCs to overcome the limits of conventional spectral broadening schemes targeting few-cycle pulses. Our approach allows for large compression ratios while maintaining high transmission, excellent beam quality, and SPM-dominated spectral broadening, even at a large spectral bandwidth, supporting few-cycle pulse durations at high repetition rates. The observed restrictions on pulse duration and spectral bandwidth can be circumvented by further improving the coating design of the cell mirrors. The precise dispersion engineering approach presented here has the potential to even extend the application range of MPCs beyond self-phase modulation and toward other nonlinear processes such as soliton [23] and dispersive wave [24] generation, four-wave mixing, and nonlinear frequency shifting [25].

Funding. Deutsche Forschungsgemeinschaft; SFB-925 (170620586); Cluster of Excellence Advanced Imaging of Matter; Helmholtz Association (HIRS-0018, VH-NG-1603); Partnership for Innovation, Education and Research (PIER) (PIF-2021-03).

Acknowledgments. We acknowledge the support of Deutsches Elektronen-Synchrotron (DESY, Hamburg, Germany), Helmholtz-Institute Jena (Germany), members of the Helmholtz Association HGF and Klas Pikull for the technical support.

Disclosures. The authors declare no conflicts of interest.

Data availability. Data underlying the results presented in this paper are not publicly available at this time but may be obtained from the authors upon reasonable request.

Supplemental document. See Supplement 1 for supporting content.

REFERENCES

1. M. Müller, A. Klenke, A. Steinkopff, H. Stark, A. Tünnermann, and J. Limpert, Opt. Lett. **43**, 6037 (2018).
2. T. Nagy, S. Hädrich, P. Simon, A. Blumenstein, N. Walther, R. Klas, J. Buldt, H. Stark, S. Breitkopf, P. Jójárt, I. Seres, Z. Várallyay, T. Eidam, and J. Limpert, Optica **6**, 1423 (2019).
3. Y.-G. Jeong, R. Piccoli, D. Ferachou, V. Cardin, M. Chini, S. Hädrich, J. Limpert, R. Morandotti, F. Légaré, B. E. Schmidt, and L. Razzari, Sci. Rep. **8**, 11794 (2018).
4. C. Grebing, M. Müller, J. Buldt, H. Stark, and J. Limpert, Opt. Lett. **45**, 6250 (2020).
5. A.-L. Viotti, M. Seidel, E. Escoto, S. Rajhans, W. P. Leemans, I. Hartl, and C. M. Heyl, Optica **9**, 197 (2022).
6. M. Hanna, F. Guichard, N. Daher, Q. Bournet, X. Délen, and P. Georges, Laser Photonics Rev. **15**, 2100220 (2021).
7. M. Müller, J. Buldt, H. Stark, C. Grebing, and J. Limpert, Opt. Lett. **46**, 2678 (2021).
8. S. Hädrich, E. Shestaev, and M. Tschernajew, *et al.*, Opt. Lett. **47**, 1537 (2022).
9. P. Balla, A. B. Wahid, and I. Sytcevich, *et al.*, Opt. Lett. **45**, 2572 (2020).
10. M.-S. Tsai, A.-Y. Liang, C. L. Tsai, P.-W. Lai, M.-W. Lin, and M.-C. Chen, Sci. Adv. **8**, eabo1945 (2022).
11. R. Piccoli, J. M. Brown, Y.-G. Jeong, A. Rovere, L. Zanotto, M. B. Gaarde, F. Légaré, A. Couairon, J. C. Travers, R. Morandotti, B. E. Schmidt, and L. Razzari, Nat. Photonics **15**, 884 (2021).
12. B. Kshirsagar and A. A. Koser, *AIP Conference Proceedings 2100*, 020200 (2019).
13. G. Millot and P. Tchofo-Dinda, "*Encyclopedia of Modern Optics: Optical Fiber Solitons, Physical Origin and properties*," Elsevier, 56–65 (2005).
14. J. Limpert, T. Schreiber, S. Nolte, H. Zellmer, and A. Tünnermann, Opt. Express **11**, 3332 (2003).
15. D. G. Ouzounov, C. J. Hensley, A. L. Gaeta, N. Venkateraman, M. T. Gallagher, and K. W. Koch, Opt. Express **13**, 6153 (2005).
16. A. Suda, M. Hatayama, K. Nagasaka, and K. Midorikawa, Appl. Phys. Lett. **86**, 111116 (2005).
17. K. F. Mak, M. Seidel, O. Pronin, M. H. Frosz, A. Abdolvand, V. Percak, A. Apolonski, F. Krausz, J. C. Travers, and P. S. J. Russell, Opt. Lett. **40**, 1238 (2015).
18. E. Escoto, A.-L. Viotti, S. Alisauskas, H. Tünnermann, I. Hartl, and C. M. Heyl, J. Opt. Soc. Am. B **39**, 1694 (2022).
19. D. Grischkowsky and A. C. Balant, Appl. Phys. Lett. **41**, 1 (1982).
20. S. Gröbmeyer, K. Fritsch, B. Schneider, M. Poetzelberger, V. Pervak, J. Brons, and O. Pronin, Appl. Phys. B **126**, 159 (2020).
21. M. Hanna, X. Délen, L. Lavenu, F. Guichard, Y. Zaouter, F. Druon, and P. Georges, J. Opt. Soc. Am. B **34**, 1340 (2017).
22. D. Herriott, H. Kogelnik, and R. Kompfner, Appl. Opt. **3**, 523 (1964).
23. R. Safaei, G. Fan, O. Kwon, K. Légaré, P. Lassonde, B. E. Schmidt, H. Ibrahim, and F. Légaré, Nat. Photonics **14**, 733 (2020).
24. J. C. Travers, T. F. Grigorova, C. Brahms, and F. Belli, Nat. Photonics **13**, 547 (2019).
25. P. Balla, H. Tünnermann, S. H. Salman, M. Fan, M. Mecejus, I. Hartl, and C. M. Heyl, Nat. Photonics **17**, 187 (2023).